

The Future Evolution of White Dwarf Stars Through Baryon Decay and Time Varying Gravitational Constant

Jacob A. Ketchum¹ • Fred C. Adams^{1,2}

© Springer-Verlag ●●●●

Abstract Motivated by the possibility that the fundamental “constants” of nature could vary with time, this paper considers the long term evolution of white dwarf stars under the combined action of proton decay and variations in the gravitational constant. White dwarfs are thus used as a theoretical laboratory to study the effects of possible time variations, especially their implications for the future history of the universe. More specifically, we consider the gravitational constant G to vary according to the parametric relation $G = G_0(1 + t/t_\star)^{-p}$, where the time scale t_\star is the same order as the proton lifetime t_P . We then study the long term fate and evolution of white dwarf stars. This treatment begins when proton decay dominates the stellar luminosity, and ends when the star becomes optically thin to its internal radiation.

Keywords stars: white dwarfs, Hertzsprung-Russell Diagram

1 Introduction

One of the overarching but unresolved questions in physics is whether or not the fundamental constants are truly constant, or if they could vary with time. A related question is whether these constants could, in principle, have other values in far-away regions of space-time (i.e., in effectively other universes). Current experiments place limits on the time variations of the fundamental constants, e.g., the gravitational constant

G and the fine-structure constant α_E (Uzan 2003 and references therein). These constraints can be expressed in terms of corresponding time scales, $\tau_G = G/\dot{G}$ and $\tau_E = \alpha_E/\dot{\alpha}_E$, which are found in the range $10^{10} - 10^{12}$ yr (Uzan 2003). Although these time scales are safely longer than the current age of the universe ($t_0 = 13.7$ Gyr; e.g., Spergel et al. 2007), these values are much shorter than some time scales that are experimentally accessible; as one example, the proton lifetime has a measured lower bound of 10^{33} yr (Super-K 1999). As a result, over the vast expanses of time available to the universe in the future, time variations in the physical constants could change the projected future history of the universe.

This paper addresses this issue by considering possible time variations of the gravitational constant and its corresponding effects on the long term evolution of white dwarf stars. In this context, we are using white dwarfs as a theoretical laboratory to consider the effects of time-varying G . This choice is justified because white dwarfs are among the simplest and hence most well understood stellar objects (starting with Chandrasekhar 1939) and because they play an important role in the future history of the universe (Adams & Laughlin 1997, hereafter AL97; see also Cikovic 2003, Dyson 1979, Islam 1977). For example, almost all stars turn into white dwarfs after their nuclear burning phase, and hence a sizable fraction of the accessible baryonic content of the universe is locked up in white dwarfs after stellar evolution has run its course (for completeness, note that a sizable fraction of the baryons remain in the medium between galaxies in dusts, e.g. Nagamine & Loeb 2004).

To address this issue, we must define both the time scales and the functional form of the time variations under consideration. Although an enormous variety of time variations are possible, we narrow the scope by allowing the gravitational constant G to vary according

Jacob A. Ketchum

Fred C. Adams

¹Michigan Center for Theoretical Physics
Physics Department, University of Michigan, Ann Arbor, MI 48109

²Astronomy Department, University of Michigan, Ann Arbor, MI 48109

to the parametric relation

$$G(t) = G_0(1 + t/t_\star)^{-p}, \quad (1)$$

where G_0 is the current value, and where t_\star and p are parameters. This functional form is perhaps the simplest type of allowed time variation — the value of G reduces to the current value at the current cosmological epoch and decreases as a power-law in the long term future. Note that current experimental limits imply that $\tau_G = G/\dot{G} > 10^{12}$ yr (e.g., Table IV of Uzan 2003; see also Barrow 1996) so that $t_\star \gg t_0$. In the long term future, proton decay is one of the most important energy sources for white dwarfs. This problem thus has two time scales of interest: the proton lifetime t_P and the time scale t_\star for variations in G . In the limit $t_\star \gg t_P$, white dwarf evolution closely follows previous results obtained using a fixed gravitational constant (AL97, Adams et al. 1998; Dicus et al. 1982). As a result, this paper primarily considers the limit $t_\star \ll t_P$, where white dwarf evolution is dominated by changes in gravity, and the case where t_\star is comparable to t_P .

Although this work will focus on time variations in the gravitational constant G , for completeness we note that time variations in other physical quantities are possible. For example, the masses of the fundamental particles or, equivalently, the ratio of electron to proton mass $\mu = m_e/m_P$, could be time dependent (Calmet & Fritzsche 2006). We note that the quark masses, which play a role in determining the proton mass, are actually the fundamental constants of the underlying theory; however, the ratio μ has been experimentally constrained (see Uzan 2003 and references therein).

In this paper we consider the variation of G by itself in order to isolate the effects of its possible time evolution. However, fundamental theories (string theory, M theory) suggest that the forces are unified and hence may vary in strength in a coupled manner (Uzan 2003 provides a brief review of the possibilities). Unfortunately, we do not have a definitive working theory of how such coupled time variations are expected to occur, and we leave such a more comprehensive treatment for future work.

This paper is organized as follows. In §2, we outline a basic model for white dwarf structure, including our treatment of time variations in G and proton decay. One interesting complication is that proton decay leads to a downward cascade for the atomic weights of the constituent nuclei; this issue is addressed in some detail. In §3 we outline the basic results of the paper, including the H-R diagrams for the long term evolution of these degenerate stars and their corresponding chemical evolution. We then conclude in §4 with a summary and discussion of our results.

2 White Dwarf Model

2.1 Conditions and Assumptions

Given the extremely long time scales associated with baryon decay and possible time variations of the gravitational constant, we make the following assumptions about the properties of the white dwarf stars under consideration here. The end of conventional star formation is expected to occur around $\sim 10^{14}$ yr after the big bang (AL97), and baryon decay will not occur until a cosmic age of $\sim 10^{33}$ yr (Super-K 1999) or later. As a result, we can safely assume that the white dwarfs will cool to low temperatures. Over time scale $10^{14} - 10^{22}$ yr they will be kept warm through dark matter capture and annihilation (AL97), but afterwards have only proton decay as an energy source. Also, any angular momentum the white dwarfs may have acquired during formation will be lost, leaving a body free of rotational deformations. As a result, electron degeneracy pressure alone must act to counterbalance gravity and maintain the star's structure against gravitational collapse.

For white dwarf stars in the low temperature limit, as considered herein, the physical structure of the star decouples from thermal considerations. We can thus assume that the equation of state is that appropriate for non-relativistic degenerate matter, so that the pressure is related to the density by the relation

$$P = K\rho^{5/3}, \quad (2)$$

where the constant K is given by

$$K = \frac{\hbar^2}{5m_e} (3\pi^2)^{2/3} (m\mu_e)^{-5/3}, \quad (3)$$

where m_e is the electron mass and m is the atomic mass unit (Shapiro & Teukolsky 1983). Here, we take $\mu_e \equiv \langle A/Z \rangle$, the average ratio of atomic mass to atomic number for the entire collection of particles comprising the white dwarf star. This ratio will be a function of time due to the effects of baryon decay (see §2.3.)

The star must be in hydrostatic equilibrium, which is described by the Lane-Emden equation, a dimensionless differential equation of the form

$$\frac{1}{\xi^2} \frac{d}{d\xi} \xi^2 \frac{d\theta}{d\xi} = -\theta^n, \quad (4)$$

where

$$r = a\xi,$$

$$\rho = \rho_c \theta^n,$$

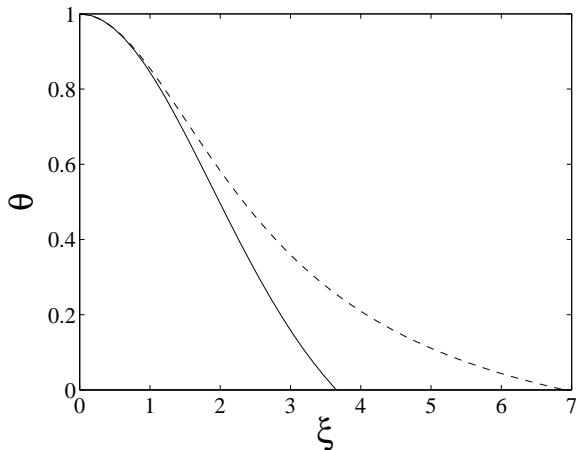


Fig. 1 Dimensionless form of the density profile given by the Lane-Emden equation for polytropic index $n = 3/2$ (non-relativistic, *solid line*) and $n = 3$ (relativistic, *dashed line*). Note that $\rho \propto \theta^n$.

and

$$a = \left[\frac{(n+1)K\rho_c^{(1/n-1)}}{4\pi G} \right]^{1/2}.$$

In this model, the white dwarf star is a polytropic, self-gravitating gas, with polytropic index $n = 3/2$. Figure 1 shows the density profile of such an idealized white dwarf for the non-relativistic case ($n = 3/2$). For comparison, the relativistic case ($n = 3$) is also shown. Note that white dwarfs are characterized by $n = 3$ (relativistic) polytropes only for masses approaching the Chandrasekhar mass; the vast majority of white dwarfs produced by the universe will have lower masses and can be described as $n = 3/2$ polytropes (e.g., Shapiro & Teukolsky 1983).

The Lane-Emden equation provides a satisfactory description for the pressure gradient in the interior of the system where the pressure is extremely high. However, once the star has radiated away all of its residual thermal energy, its surface temperature will be nearly absolute zero. For the outer layers of a frozen white dwarf, the typical inter-particle separation is about one Bohr radius, and the constituent particles naturally fall into a tightly packed lattice structure. This densely packed state for the matter in a frozen white dwarf effectively places a positive, non-zero lower bound on the density. Here, we take the lower bound on the density of this lattice to be a constant value $\rho_0 = 1 \text{ g cm}^{-3}$. At this density the coulomb, self-gravitational, and degeneracy energies have comparable magnitudes and the electrons are no longer degenerate.

Early in a white dwarf's lifetime, this non-degenerate surface layer is extremely thin, with little of the stellar

mass residing therein, and it is a reasonable approximation to assume that the entire system is degenerate. For instance, early in the life of a $1.0 M_\odot$ white dwarf, the non-degenerate 'crust' is only about 1 km deep. On the time scales of this paper, as the star expands due to mass loss from proton decay and varying G , it is essential to follow the boundary between degenerate and non-degenerate layers within the white dwarf.

2.1.1 Mass

The total remaining mass of the white dwarf at any time is given by the equation

$$M(t) = M_0 \exp[-\Gamma t], \quad (5)$$

where Γ is the baryon decay rate. For the sake of definiteness, we take $\Gamma = 10^{-37} \text{ yr}^{-1}$ for this work; the issue of proton lifetimes is discussed in §2.2.

Invoking conservation of mass and the definitions of equation (4), the mass contribution of the degenerate core enclosed within the degenerate surface, ξ_{deg} , is given by

$$M_{deg}(t) = \eta_m [\rho_c(t) G(t)^{-3} \mu_e(t)^{-5}]^{1/2}, \quad (6)$$

where

$$\eta_m = \frac{1}{4\sqrt{2}\pi} \left(\frac{\hbar^2}{m_e} (3\pi^2)^{2/3} m^{-5/3} \right)^{3/2} \xi_{deg}^2 |\theta'_{deg}|.$$

An alternative way of calculating the total mass is to substitute ξ_1 and $|\theta'_1(\xi_1)|$ for ξ_{deg} and $|\theta'_{deg}|$, respectively, for the expression η_m in equation (6), effectively adding up the mass of a completely hydrostatic polytropic gas,

$$\mathcal{M} = \eta_{\mathcal{M}} \frac{M_{deg}}{\eta_m}, \quad (7)$$

where

$$\eta_{\mathcal{M}} = \eta_m \frac{\xi_1^2 |\theta'_{\xi_1}|}{\xi_{deg}^2 |\theta'_{deg}|}.$$

The mass contribution M_{ndeg} due to non-degenerate material is given by the difference between equations (5) and (6),

$$M_{ndeg} = M - M_{deg}. \quad (8)$$

We keep track of the time evolution for all three quantities in our analysis of white dwarf evolution. Of particular interest is the epoch when $M_{deg} = M_{ndeg}$, a time that we define as the end of the white dwarf's degenerate phase.

2.1.2 Radius

The radius of the degenerate core is given by

$$R_{deg}(t) = \eta_r [\rho_c(t) G^3(t) \mu_e^5(t)]^{-1/6}, \quad (9)$$

where

$$\eta_r = \frac{1}{2\sqrt{2\pi}} \left(\frac{\hbar^2}{m_e} (3\pi^2)^{2/3} m^{-5/3} \right)^{1/2} \xi_{deg}.$$

Adding the radial contribution of the non-degenerate shell, we find an overall white dwarf radius of

$$R(t) = \left[\frac{3M_{ndeg}}{4\pi\rho_0} + R_{deg}^3 \right]^{1/3}. \quad (10)$$

Since the contribution to the overall radius due to non-degenerate matter is small early on (only 0.05% for our adopted lower bound on density $\rho_0 = 1 \text{ g cm}^{-3}$), an approximate form is obtained by substituting ξ_1 for ξ_{deg} in η_r of equation (9). This approximation effectively assumes that the full, non-truncated density description is given by the Lane-Emden equation, so that

$$\mathcal{R} = \eta_{\mathcal{R}} \frac{R_{deg}}{\eta_r}, \quad (11)$$

and

$$\eta_{\mathcal{R}} = \eta_r \frac{\xi_1}{\xi_{deg}}.$$

Because we set a lower bound ρ_0 on the density at the outer surface, the overall radius R is always less than \mathcal{R} , the radius obtained without assuming a minimum density. Calculations of surface temperature in this work (see §2.1.4) use the radial equation (10), whereas previous calculations (Adams et al. 1998) used the radial form given by (11).

2.1.3 Central Density

At this point we have expressions for the total mass and total radius of the white dwarf, where we have included a lower bound ρ_0 on the density. However, both the degenerate mass and radius depend on the central density of the white dwarf. The ratio of average density to central density of a polytropic system is given by

$$\frac{\bar{\rho}}{\rho_c} = \frac{3|\theta'(\xi_1)|}{\xi_1}, \quad (12)$$

where here the average density is described in terms of the non-truncated mass (7) and radius (11), *i.e.*,

$$\bar{\rho} = \frac{\mathcal{M}}{4/3\pi\mathcal{R}^3}. \quad (13)$$

Note that this average density represents that corresponding to the entire profile given by the Lane-Emden equation, not a profile that is truncated at some non-zero density. It is also useful in evaluating equation (13) to invoke the mass-radius relation

$$\mathcal{M}\mathcal{R}^3 = \eta_{\mathcal{R}}^3 \eta_{\mathcal{M}} G^{-3} \mu_e^{-5}.$$

Putting these results together, we find that the central density of the white dwarf can be expressed by the following function of time alone,

$$\rho_c(t) = \eta_{\rho} [M^2(t) G^3(t) \mu_e^5(t)], \quad (14)$$

where

$$\eta_{\rho} = \left(\frac{\xi_1}{4\pi|\theta'(\xi_1)|} \right) \frac{1}{\eta_{\mathcal{R}}^3 \eta_{\mathcal{M}}}.$$

This form provides the correct central density for the white dwarf while a degenerate core is present (otherwise $\rho_c = \rho_0$).

2.1.4 Luminosity and Temperature

The luminosity of the white dwarf is provided by proton decay and is given by

$$L(t) = \mathcal{F}c^2\Gamma M(t), \quad (15)$$

where $\mathcal{F} \approx 2/3$ is an efficiency factor ($\mathcal{F} \leq 1$ due to neutrino losses, since such particles do not thermalize within the star). The surface temperature of the star is given by

$$T^4(t) = \frac{L(t)}{4\pi\sigma_{sb}R^2}, \quad (16)$$

where σ_{sb} is the Stephan-Boltzmann constant, and R is the radius given by equation (10). Given that $R \leq \mathcal{R}$, the effect of including a lower bound on density is to provide the star with a somewhat higher temperature, effectively shifting its trajectory in the HR diagram to the left during late times.

2.2 Proton Decay

Proton decay has many possible channels, but the most relevant possible processes can be conceptually divided into two types. The first type of process takes place through unification scale effects, where the intermediate particle that drives decay is a GUT scale particle that violates baryon number conservation. The second type of process is driven by gravitational effects. In this case, the simplest description invokes virtual black holes, which also violate baryon number conservation,

as the effective intermediate particles (for completeness we note that string theories render this description overly simplistic). In either case, the estimated time scale for proton decay is given approximately by the expression

$$t_P = \tau_c \left(\frac{M_X}{m_P} \right)^4, \quad (17)$$

where $\tau_c \sim 10^{-31}$ yr is the light crossing time of the proton, m_P is the proton mass, and M_X is the mass of the intermediate particle that drives the decay process.

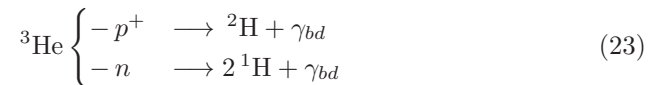
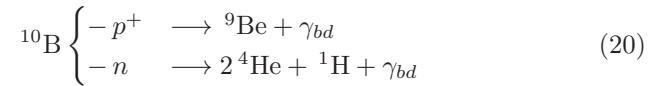
For the case of GUT scale proton decay, $M_X \sim M_{GUT} \sim 10^{16}$ GeV; in this case, the proton decay time scale is about 10^{33} yr, roughly the same as the current experimental bounds (Super-K 1999). For the case of gravitational proton decay, one expects $M_X \sim M_{Pl} \sim 10^{19}$ GeV. This value for the intermediate particle mass implies a proton decay time scale of about 10^{45} yr, much longer than current bounds. Since the suppression of baryon number violation at the Planck scale is difficult, we expect the proton lifetime to fall in the range 10^{33} yr $\leq t_P \leq 10^{45}$ yr. For the sake of definiteness, we take an intermediate time-scale between these limits as a working benchmark value so that $\Gamma^{-1} \sim t_P \sim 10^{37}$ yr.

For the case of gravitationally driven proton decay with time varying G , an additional complication arises. The Planck mass, which sets the effective scale for the virtual black holes, scales as $M_{Pl} \propto G^{-1/2}$, so the (gravitationally driven) proton decay time scales as $t_P \propto G^{-2}$. As a result, the proton lifetime is expected to increase as the gravitational constant decreases.

2.3 Chemical Cascade Chain

This section investigates the variations of $\mu_e \equiv \langle A/Z \rangle$, which determines, in part, the equation of state. This quantity changes with time due to nuclear decay events that determine the long term fate of white dwarf stars. Initially, a white dwarf star will most likely consist of a mixture of heavier elements such as ${}^4\text{He}$, ${}^{12}\text{C}$, and ${}^{16}\text{O}$. On sufficiently long time scales, however, random baryon decay events send these particles on a cascading path towards ${}^1\text{H}$, and eventually total extinction. To first order, μ_e is proportional to the mean value $\langle A/Z \rangle$ of the white dwarf's constituent elements. This ratio will be nearly 2 for any white dwarf consisting mostly of heavier elements. By the time that about half of the original nucleons have decayed through proton decay processes, however, a significant portion of the composite mass will be in the form of Hydrogen, for which $\mu_e = 1$. We thus expect μ_e to be a decreasing function of time, with $\mu_e \rightarrow 1$ in the long time limit $t \rightarrow \infty$.

This cascade of particles is categorized below. This chain begins with ${}^{12}\text{C}$, and continues down to baryonic extinction (Thornton & Rex 2000); note that we could start with larger nuclei (e.g. Oxygen), but the latter parts of the chain would remain the same. The basic reactions include:



These reaction equations show the nuclei resulting from each particular baryon decay event and an energy release. Each reaction given above may actually include several different reactions en route to the production of the listed stable particles. Among the decay products will be some particle with a positive charge, often a positron, which annihilates with an electron and turns into energy represented by the photons γ_{bd} in the reaction equations. Among the baryon decay events listed above, (b) signifies either a proton or a neutron decaying, (n) signifies neutron decay, and (p^+) signifies proton decay. The particular daughter particles for ${}^{10}\text{B}$ and ${}^3\text{He}$ are dependent upon whether a proton or a neutron decays, whereas the other particles listed in the chain produce only one variety of products, regardless of whether a proton or a neutron decays. Although most reactions listed above have outcomes that are independent of which particle decays, the exact path taken to achieve the stable particles could vary (and are not documented in the chain).

To model this process, we used a Monte Carlo simulation to follow the evolution of the particle species population as a function of overall mass for a white

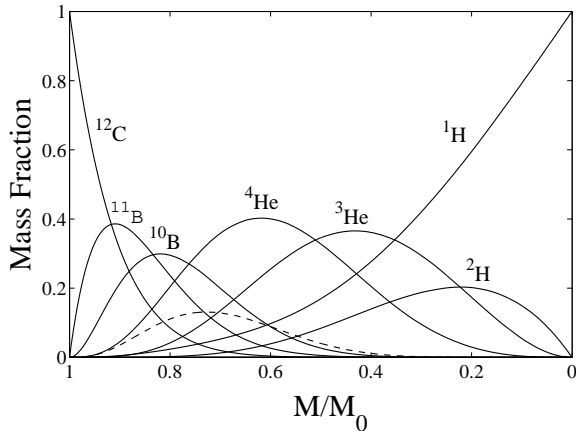


Fig. 2 Chemical species mass fraction versus relative mass of white dwarf with initial composition of pure ^{12}C . Each curve represents a species of particle within the white dwarf during proton decay. The labels indicate the particle species, with the exception of ^9Be , which is represented by the dashed curve.

dwarf star undergoing baryonic decay. In these simulations, both protons and neutrons were allowed to decay with equal likelihood; since proton decay (neutron decay in bound nuclei) has not yet been measured, this assumption remains unverified experimentally. If the resultant nucleus is unstable to decay, then the decay was immediately allowed to take place (since the proton decay time-scale is far greater than the nuclear decay time-scale of any known isotopes of light elements.) Figure 2 shows the results of one such Monte Carlo simulation for an initial collection of $\sim 10^6$ atoms of ^{12}C , which were subject to baryon decay (see also AL97). The implications of this chemical cascade on the values of μ_e , and hence the equation of state, are discussed below.

For completeness, we note that the values of μ_e can be affected by spallation and pycnonuclear reactions. In particular, pycnonuclear reactions work to build up the abundance of ^4He from smaller elements, effectively widening and raising the ^4He curve of Figure 2 at the expense of the ^3He , ^2H , and ^1H curves. The effect is to increase the value of μ_e and hence the height of the curve in Figure 3 near the low mass end. Spallation events slowly redistribute protons and neutrons one at a time among the nuclei in the star. This redistribution happens at a rate that is approximately one per baryon decay event. Thus, spallation has a similar effect as pycnonuclear reactions in that it acts to increase the size of the nuclei, albeit at a slow rate, and slightly increases the value of μ_e near the end of the white dwarf's life.

Figure 3 shows the ratio μ_e as a function of time, where time is given in terms of the white dwarf mass.

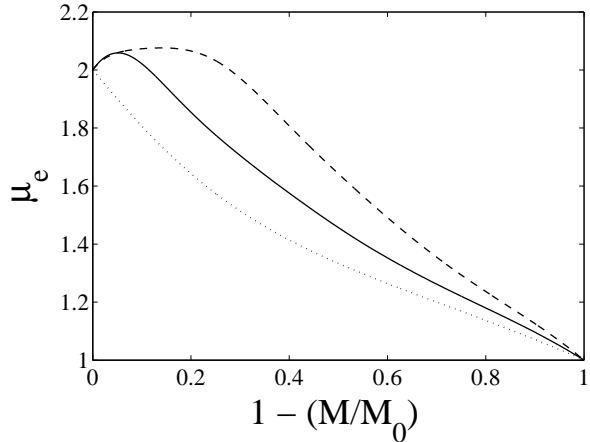


Fig. 3 The ratio μ_e as a function of decayed mass fraction for white dwarf compositions of initially pure ^{16}O (dashed), ^{12}C (solid), and ^4He (dotted).

These curves are calculated from the Monte Carlo simulations described earlier. Initially $\mu_e = 2$ for all three curves, corresponding to their respective homogeneous compositions. For a brief period for the ^{12}C curve, this ratio rises above 2 to an approximate value of 2.06 with nearly 95% of the initial mass remaining. This ratio then decreases monotonically towards a value of 1 (homogeneous ^1H composition). The ^{16}O curve has a much broader hump above the $\mu_e = 2$ line and reaches a maximum value of approximately 2.07 with nearly 86% of the initial mass remaining. These curves would rise slightly between the end points by including spallation and pycnonuclear effects in the Monte Carlo simulation.

For simplicity, we use a fitting function that represents the μ_e curves of Figure 3 with an accuracy of $\sim 1\%$. The fitting function has the form

$$\mu_e(u) = 2 - u + (a_1 u + a_2 u^2 + a_3 u^3) \exp(a_4 u), \quad (26)$$

where $u = 1 - M/M_0$. Although one can find a good fit to these curves, there exists no unique set of fitting parameters (a_1, a_2, a_3, a_4) . Clearly, $a_1 + a_2 + a_3 = 0$ in order to fulfill the requirement that $\mu_e(1) = 1$. But, more specifically, for a given a_4 , there exists no unique pair (a_1, a_2) that provides a fit to within a given accuracy. In Table 1 we provide suggested fitting parameters for three different cases where the initial white dwarf composition is taken to be of pure ^4He , ^{12}C , or ^{16}O (note that we give a large number of significant figures in this table).

Table 1 Fitting parameters for μ_e time evolution curves. The Monte Carlo simulations were started with a pure concentration of the chemical species listed in the left column. The time evolutions of μ_e are recovered by substituting the parameters from this table into equation (26).

Species	a_1	a_2	a_3	a_4
^4He	-0.952	3.23	4.182	-3.025
^{12}C	3.1218	-12.9250	9.24125	-4.95509
^{16}O	1.8935	14.3400	-16.2335	-5.6545

3 Results

Given the model for white dwarf structure constructed in the previous section, we consider the long term evolution of these degenerate stars through the action of proton decay and time varying gravitational constant. To start, we first consider the case where gravity varies but no proton decay takes place. Under these conditions, the white dwarf grows in radial size with time. Both the radius of the degenerate interior and the fraction of the star that makes up the non-degenerate outer layer are increasing functions of time.

The overall radius increases for two reasons: (1) reducing gravity’s strength effectively reduces the central density of the white dwarf, allowing the degenerate core to spread out, and (2) the reduction of the degenerate core mass results in an increase in mass of the frozen solid lattice (approximately at constant density), leading to an increase in its radius. If gravity weakens enough, the pressure exerted by gravity at the center of the white dwarf decreases below the $\sim 10^{12}$ dyne cm^{-2} lower bound, completely dissolving the degenerate core into the outer solid lattice. In the long term, the white dwarf is left with a radial density that is practically uniform and a maximal surface radius. Figure 4 shows the radius as a function of time for this scenario with different rates of gravitational time scales t_* for a $1M_\odot$, white dwarf with pure ^{12}C composition. This figure shows that under gravitational time variations, the white dwarf grows to nearly 100 times its original radius before becoming a frozen lattice composed fully of non-degenerate matter.

We also consider the case of constant gravity while subjecting the star to baryon decay, which causes the star to lose mass. The white dwarf increases in radial size until its mass in degenerate matter decreases to only about two thirds of the total stellar mass. After this point, the radius and mass of the white dwarf shrink until the internal coulomb forces dominate over gravity, and the object resembles a rock. This scenario is captured by the red curves in Figures 5, 6, 7, and 8.

Next we consider the effects of both time variations in the gravitational constant and baryon decay. The

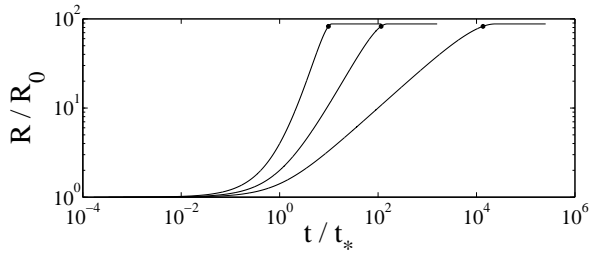


Fig. 4 Radius versus time diagram for white dwarf evolution with constant ^{12}C composition (*no baryon decay*) and time varying G with $t_* = 10^{37}$ yr; $p = 0.5$ (*right*), 1.0 (*middle*), and 2.0 (*left*). The mass is $1M_\odot$. Radius and time are shown in dimensionless form. The dots mark the end of the white dwarf’s degenerate phase. In all three cases the white dwarf grows to almost 100 times its original radius, but the time scale on which this growth occurs varies with p .

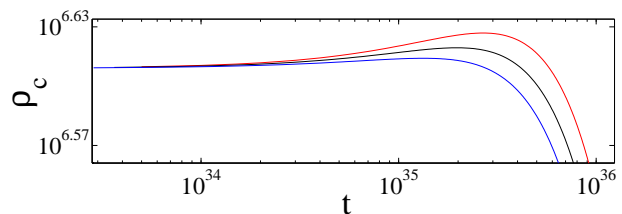


Fig. 5 Central density versus time for white dwarf evolution with initial ^{12}C composition and $\Gamma^{-1} = t_* = 10^{37}$ yr; $p = 0.0$ (*red*), 0.25 (*black*), and 0.5 (*blue*). The starting mass is $1M_\odot$. Notice that the central density increases before falling off rapidly for all three cases. This feature of the central density is due to the initial increase in μ_e for ^{12}C and thus is expected to occur for an ^{16}O white dwarf as well. Density is shown in g cm^{-3} and time is given in years.

interplay between these two effects will be the focus of the remainder of this section. As shown below, the main result is to reduce the ratio of degenerate to non-degenerate matter within the star at the time when the remnant begins its shrinking phase.

Figures 6 and 7 show the time behavior of mass and radius, respectively, for a $1.0 M_\odot$ white dwarf composed initially of pure ^{12}C , subjected to baryonic decay with characteristic time scale of $\Gamma = 10^{-37} \text{ yr}^{-1}$. The three different sets of curves represent various indices of gravitational weakening with time constant $t_* = 10^{37}$ yr. In Figure 6, one can see that the overall mass envelope (*solid line*) for a white dwarf under these conditions is independent of the gravitational index p and is fully described by Γ , the characteristic time for baryon decay. The set of red curves show the case of a static gravitational constant ($p = 0$). As baryons decay, more material precipitates out of the degenerate core (*dashed line*) to join the outer, non-degenerate layer (*dotted line*). At

time $t \approx 5.4 \times 10^{37}$ yr ($\Gamma t = 5.4$), nearly 99.5% of the white dwarf's initial mass has decayed and the mass in the degenerate core is less than the mass in the non-degenerate outer lattice. This event is marked by the solid, red triangles in Figures 6, 7, and 8, and marks the time when the degenerate phase of the star comes to an end. This event does not spell the end of the white dwarf's life, which goes well beyond $t \approx 5.9 \times 10^{37}$ yr ($\Gamma t = 5.9$) when the degenerate core disappears entirely from the stellar remnant. As shown in Figure 7, this time also approximately marks the point when the star begins to shrink in radius. At this epoch, $R \approx 1.2 \times 10^5$ km, a size that is comparable to that of Uranus or Neptune.

Figure 8 shows the H-R diagram, which summarizes the evolution of these white dwarf stars. While the star remains (mostly) degenerate, the tracks in the H-R diagram are approximately given by $L \sim T^{12/5}$. This form would be exact for an object that obeys the usual white dwarf (degenerate) mass-radius relation and has luminosity proportional to its mass. Moderate deviations from this simple behavior occur due to variations in the chemical composition, which affect the equation of state (and due to time variations in G – see below). After the degenerate phase ends, the tracks in the H-R diagram become much steeper with $L \sim T^{12}$. This form applies for a constant density object with its luminosity proportional to its mass. At this transition point, 99.5% of the mass has decayed away, the chemical composition for this white dwarf is $\sim 99\%$ ^1H , $\sim 1\%$ ^2H , with traces of ^3He and ^4He (see Figure 3). The remnant now amounts to a medium sized planet, composed mostly of Hydrogen ice, glowing extremely dim with an output of only ~ 2 Watts (Figure 8). This huge ball of Hydrogen ice fizzes away as the white dwarf continues to fade and shrink. Finally, around 2.2×10^{38} yr ($\Gamma t = 22$), when the mass is $\sim 10^{21}$ kg, radius $R = 2.9 \times 10^2$ km, effective temperature is $T = 1.3 \times 10^{-3}$ K, and luminosity $L = 1.9 \times 10^{-7}$ Watts, the remnant ceases to be a star.

This story changes only slightly with the introduction of a time varying gravitational constant. The set of black curves in these Figures shows what happens when the gravitational index is $p = 0.25$, and blue curves represent a gravitational index $p = 0.5$. For the scenario where $p = 0.25$, the degenerate phase ends at $t \approx 4.8 \times 10^{37}$ yr ($\Gamma t = 4.8$) when 99.1% of the mass has decayed away. At this time, the star is about 1.5×10^5 km in radius and has a power output of about 3.3 Watts. This white dwarf is $\sim 98.2\%$ ^1H , $\sim 1.8\%$ ^2H , and $\sim 0.07\%$ ^3He by mass, and is thus nearly identical chemically to the white dwarf evolving with a static gravitational constant. For the scenario where $p = 0.5$, the degenerate phase ends at $t \approx 4.2 \times 10^{37}$ yr ($\Gamma t = 4.2$)

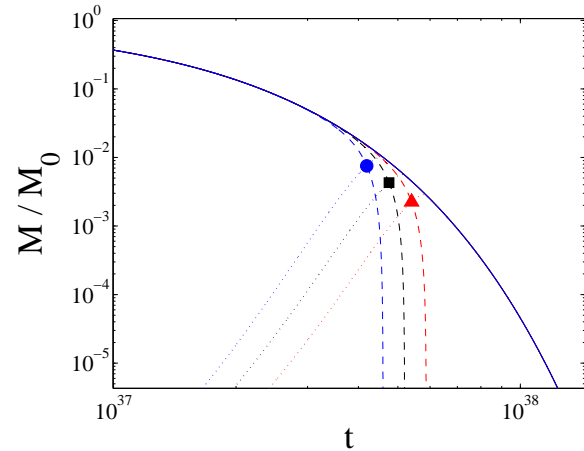


Fig. 6 Mass versus time for white dwarf evolution through proton decay with an initial ^{12}C composition and $t_* = \Gamma^{-1} = 10^{37}$ yr; $p = 0$ (red), 0.25 (black), and 0.5 (blue); $M(t)$ (solid), M_{deg} (dashed), M_{ndeg} (dotted). Mass is shown as the remaining fraction and time is shown in years. The triangle, square, and circle mark the fractional mass and time when the mass in non-degenerate form equals the amount of degenerate mass for gravitational index $p = 0$, 0.25, and 0.5, respectively. This crossover point defines the time when the white dwarf's degenerate phase ends and its non-degenerate phase begins.

when 98.5% of the mass has decayed away. At this time, the star is about 1.8×10^5 km in radius and has a power output of about 5.7 Watts. This white dwarf is $\sim 97.1\%$ ^1H , $\sim 2.7\%$ ^2H , and $\sim 0.1\%$ ^3He by mass, and is also nearly chemically identical to the white dwarf produced using a fixed gravitational constant.

The white dwarf completes its transformation into a rock of hydrogen ice when it becomes optically thin to the radiation that originates from within. This condition is determined by the star's column density. The star contains two types of radiation that must be considered when determining this transition. The first type is the ~ 235 MeV gamma rays produced in each baryon decay event; the stellar remnant becomes optically thin to this radiation at an approximate radius of 1 meter (for our assumed ρ_0). The other type is the radiation that comes from the thermalization of these gamma rays, which produce photons with wavelength $\lambda \sim 10^2$ cm. The white dwarf becomes optically thin to this radiation at a mass of about 10^{21} kg and radius of 2.9×10^2 km. This mass is calculated by using the average density of the white dwarf, a value that depends only upon coulomb forces between neighboring particles in the Hydrogen lattice and not upon gravity. As a result, the transition from white dwarf to rock for the two scenarios with $p = 0.25$ and $p = 0.50$ depends only upon Γ , and thus happens at the same time, mass, radius,

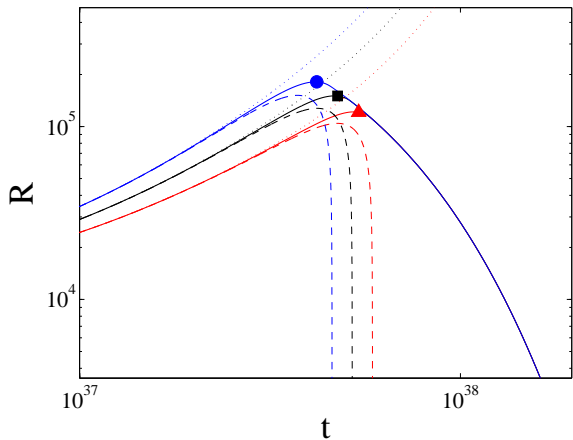


Fig. 7 Radius versus time for white dwarf evolution through proton decay with initial ^{12}C composition and $t_* = \Gamma^{-1} = 10^{37}$ yr; $p = 0$ (red), 0.25 (black), and 0.5 (blue); \mathcal{R} (dotted), R (solid), R_{deg} (dashed). Radius is shown in km and time is shown in years. The triangle, square, and circle correspond to those shapes in Figure 6. In all cases, these degeneracy transitions occur shortly after the white dwarf has reached maximum radius and has begun to shrink.

temperature, and luminosity as the case with $p = 0$. Corrections to this approximation could come from accounting for the exact chemical make up and crystal grain structure of the solid lattice, both of which would differ slightly for the three indices.

Figures 9 and 10 show curves characterizing the time and mass marking the end of the degenerate phase of the white dwarf for a continuum of gravitational indices spanning 10 orders of magnitude, and seven characteristic time scales for gravitational time variations. These graphs show the limiting behavior for $p \ll 1$ and $p \gg 1$ and for intermediate values. For instance, in the benchmark case of a pure ^{12}C white dwarf, the dynamical range of index parameter is $0.01 \leq p \leq 100$. If p takes on values lower than this range, the fate of the white dwarf is dominated by proton decay; if p takes on values larger than this range, then the fate of the white dwarf is dominated by gravitational time variations. This dynamical range of index parameters broadens and increases as the product Γt_* increases, which indicates that gravity must vary rapidly to compete with a proton decay.

Before leaving this section, we briefly consider the issue of the “starting” mass. First, note that the “starting” mass in this context is the “final” mass in stellar evolution calculations. At the end of their nuclear burning phase, stars become white dwarfs with masses in the range $0.08M_\odot \leq M \leq 1.4M_\odot$. To leading order, white dwarfs with larger masses must become white dwarfs with smaller masses as their constituent baryons

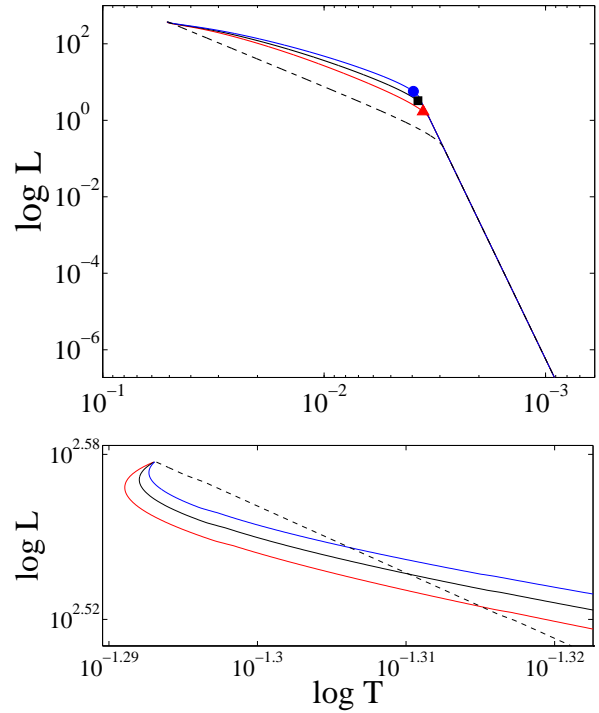


Fig. 8 H-R Diagram for white dwarf evolution including proton decay and time variations in the gravitational constant. In all cases, the star begins with mass $M = 1.0 M_\odot$, a pure ^{12}C composition, and evolves according to $t_* = \Gamma^{-1} = 10^{37}$ yr. The three curves show different values of the gravitational index $p = 0$ (red), 0.25 (black), and 0.5 (blue). Temperature is shown in Kelvin and luminosity is shown in Watts. The triangle, square, and circle correspond to those shapes in Figure 6. The dashed line shows the reference case of a white dwarf with constant $\mu_e = 2$ and no variations in the gravitational constant ($p = 0$). The lower panel shows a close-up of the beginning of the time evolution, for the first $\sim 10\%$ of the mass loss. During this early phase, $\mu_e > 2$, the radius shrinks slightly, and the photospheric temperature heats up.

decay. As a result, white dwarf evolution should not depend sensitively on the starting mass (in the long term). However, the chemical composition plays a role in determining stellar structure, primarily through the value of μ_e , which in turn determines the equation of state. White dwarfs with larger initial masses must lose a larger percentage of their mass before becoming non-degenerate, and hence will experience a greater change in chemical composition. One might expect the stellar properties at the transition point (from degenerate to non-degenerate stars) to depend on the starting stellar mass. However, the larger white dwarfs begin their evolution with larger nuclei (e.g., Carbon and Oxygen), whereas small white dwarfs (a few $0.1 M_\odot$) are made up mostly of Helium. These two effects largely compen-

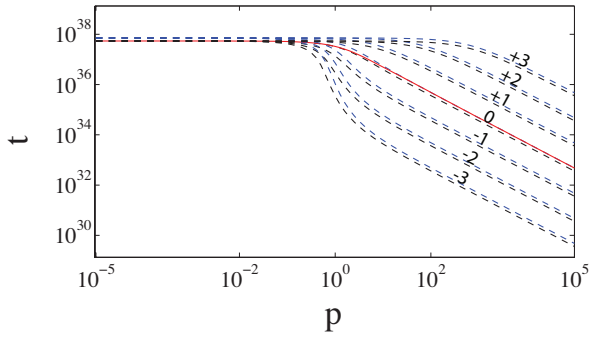


Fig. 9 Time duration of the degenerate phase of white dwarf evolution as a function of the gravitational index p . The proton decay time parameter $\Gamma = 10^{-37} \text{ yr}^{-1}$ and the gravitational strength time parameter $t_* = 10^{37} \text{ yr}$. The initial mass of the white dwarf is $1 M_\odot$. Each set of curves contains one black ($\mu_e = 1$) and one blue ($\mu_e = 2$) dashed line and are labeled by an integer $\ell = -3, -2, \dots, 3$ where $\ell = \log(\Gamma t_*)$. The time marking the end of the degenerate phase is largely independent of p when $t_* \geq \Gamma^{-1}$ and for $p < 1$. For values of $p \gg 1$, the different curves become monotonically decreasing, parallel lines. The solid curve represents a white dwarf star initially composed of pure ^{12}C .

sate, so that white dwarfs of all starting masses become non-degenerate with roughly the same properties.

To illustrate this point, consider white dwarfs subject to both baryon decay and time varying G , with the standard time scales $t_* = \Gamma^{-1} = 10^{37} \text{ yr}$ and with $p = 1$. We can then examine stellar properties at the time when the stars become non-degenerate. For a small $0.1 M_\odot$ white dwarf initially composed of ^4He , this transition occurs at $t = 1.8 \times 10^{37} \text{ yr}$ ($\Gamma t = 1.8$) when $\mu_e \approx 1.11$, the mass $M = 1.6 \times 10^{-2} M_\odot$, and the radius $R = 1.9 \times 10^6 \text{ km}$. For comparison, for a larger $1.0 M_\odot$ white dwarf initially composed of ^{12}C , this transition occurs at $t = 3.3 \times 10^{37} \text{ yr}$ ($\Gamma t = 3.3$) when $\mu_e \approx 1.03$, the mass $M = 3.8 \times 10^{-2} M_\odot$, and the radius $R = 2.45 \times 10^6 \text{ km}$. These differences are thus at the factor of ~ 2 level.

4 Conclusion

This paper has constructed a model for the structure and evolution of white dwarf stars under the action of both proton decay and time variations in the gravitational constant (section 2). This model includes variations in chemical composition (Figure 2 and section 2.3) which affects the equation of state. The model also includes separate accounting for the inner degenerate regions (which obey the polytropic equation of state [1]) and the outer non-degenerate regions.

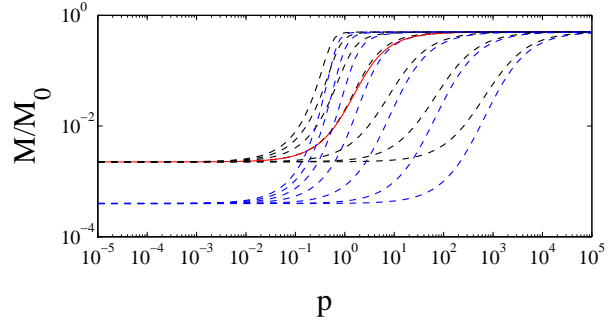


Fig. 10 Mass fraction in degenerate matter versus gravitational index p . Each set of curves contains one black ($\mu_e = 1$) and one blue ($\mu_e = 2$) dashed line and correspond to an integer $\ell = -3, -2, \dots, 3$, from left to right, where $\ell = \log(\Gamma t_*)$. The dynamical range for $\Gamma = t_*$ has p spanning 4 orders of magnitude centered at $p = 1$. The solid curve represents a white dwarf star initially composed of pure ^{12}C .

Our main findings can be summarized as follows:

In the absence of baryon decay, white dwarfs grow larger as the strength of gravity decreases (Figure 4). The radius reaches a maximum value when the entire star becomes non-degenerate; at this time, the radius is ~ 100 times larger than its starting value.

With the inclusion of baryon decay, white dwarfs lose mass with time and follow tracks in the H-R diagram as shown in Figure 8. In all cases, after an initial transient phase, the stars grow dimmer and redder with time, and hence move to the lower right in the H-R diagram. While the stars remain (primarily) degenerate, the tracks have a shallow slope, with $L \propto T^{12/5}$. After the stars lose enough mass to become primarily non-degenerate, the tracks become much steeper, with $L \propto T^{12}$. These slopes would be exact in the absence of changes in the chemical composition; the chemical variations and the time variations in G lead to small departures from this behavior.

During the degenerate regime of evolution, the radii of these white dwarf stars grow larger due to mass loss from proton decay and due to the weakening of gravity. During the later, non-degenerate phase, the radii become smaller. The maximum value of the radius occurs near the transition between the degenerate and non-degenerate regimes, with a value that is typically ~ 10 times the starting radius (see Figure 7).

In addition to understanding the long term fate and evolution of white dwarfs, one motivation for this work is to understand the larger issue of the future of the universe. Previous projections of the future (e.g. AL97, Dyson 1979) are predicated on the assumption that the laws of physics are known and will not change

with time. One important issue is thus the question of whether or not the constants of nature change with time, and how such variations would change projections of our future history. In the case of white dwarf evolution, we find that time variation leads to quantitative — but not qualitative — changes in the future timeline. Time varying G leads to variations in the exact mass, size, and composition of white dwarfs as they become non-degenerate rock-like objects. However, the starting states and final states are essentially the same, so time variations in gravity do not lead to fundamental changes in the overall picture. White dwarfs start as degenerate objects with the current value of G , and hence are constrained to begin their evolution in nearly the same states. At the other end of time, white dwarfs cease to act as stars when they become optically thin to their internal radiation. At this epoch, the “stars” are essentially large rocks of Hydrogen ice, and their structure is non-degenerate and largely independent of gravity. As a result, time variations in G primarily affect the intermediate states, and this work shows that the modifications are relatively modest (see Figures 5 - 8).

Acknowledgements We thank Jeff Druce for useful discussions. This work was supported by the Foundational Questions Institute through Grant RFP1-06-1 and by the Michigan Center for Theoretical Physics.

References

- Adams, F. C., & Laughlin, G.: A dying universe: the long-term fate and evolution of astrophysical objects. *Rev. of Mod. Phys.* **69**, 2 (1997)
- Adams, F. C., Laughlin, G., Mbonye, M., & Perry, M. J.: Gravitational demise of cold degenerate stars. *Phys. Rev. D*, **58**, 083003 (1998)
- Barrow, J. D.: Time varying G. *Mon. Not. R. Astron. Soc.* **282**, 1397 (1996)
- Barrow, J. D., & Parsons, P.: Cosmological models with varying G. *Phys. Rev. D*, **55**, 1906 (1997)
- Calmet, X., & Fritsch, H.: Time variation of electron-proton mass ratio. [astro-ph/0605232](https://arxiv.org/abs/astro-ph/0605232) (2006)
- Chandrasekhar, S.: *Stellar Structure*. (New York: Dover) (1939)
- Cirkovic, M. M.: Resource Letter: Physical eschatology. *Am. J. Phys.*, **71**, 122 (2003)
- Davies, P. C. W.: Time variation of coupling constants. *J. Phys. A.*, **5**, 1296 (1972)
- Dicus, D. A., Letaw, J. R., Teplitz, D. C., & Teplitz, V. L.: Effects of proton decay on the cosmological future. *Astrophys. J.*, **252**, 1 (1982)
- Dyson, F. J.: Time without end. *Rev. Mod. Phys.*, **51**, 447 (1979)
- Hawking, S. W.: Black hole explosions? *Nature*, **248**, 30 (1974)
- Islam, J. M.: Possible ultimate fate of the universe. *Q. J. R. Astron. Soc.*, **18**, 3 (1977)
- Nagamine, K. & Loeb, A.: Future evolution of the intergalactic medium in a universe dominated by a cosmological constant. *New Astron.*, **9**, 573 (2004)
- Shapiro, S. L., & Teukolsky, S. A.: *Black Holes, White Dwarfs, and Neutron Stars*. (Wiley & Sons) (1983)
- Spergel, D. N. et al.: WMAP three year results: Implications for cosmology. *Astrophys. J. Suppl. Ser.*, **170**, 377 (2007)
- Super-Kamiokande Collaboration: Search for proton decay through $p \rightarrow \bar{\nu}K^+$ in a large water Cherenkov detector. *Phys. Rev. Lett.*, **83**, 1529 (1999)
- Thornton, S. T., & Rex, A.: *Modern Physics for Scientists and Engineers*. (Sauders) (2000)
- Uzan, J. P.: The fundamental constants and their variation. *Rev. Mod. Phys.*, **75**, 403 (2003)
- Zel'dovich, Ya. B.: Gravitational annihilation of baryons. *Phys. Lett. A*, **59**, 254 (1976)